NASA TECHNICAL NOTE

NASA TN D-6960

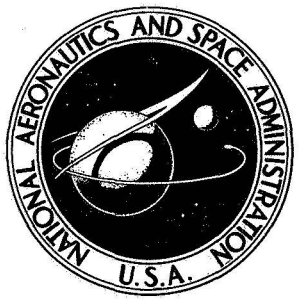

NASA TN D-6960

COLD-AIR INVESTIGATION OF A TURBINE FOR HIGH-TEMPERATURE-ENGINE APPLICATION

IV — Two-Stage Turbine Performance

by Warren J. Whitney, Harold J. Schum, and Frank P. Behning

Lewis Research Center
Cleveland, Ohio 44135

NATIONAL AERONAUTICS AND SPACE ADMINISTRATION • WASHINGTON, D. C. • SEPTEMBER 1972

COLD-AIR INVESTIGATION OF A TURBINE FOR HIGH-TEMPERATURE-ENGINE APPLICATION IV - TWO-STAGE TURBINE PERFORMANCE

by Warren J. Whitney, Harold J. Schum, and Frank P. Behning

Lewis Research Center

SUMMARY

The performance of the two-stage, 0.6604-meter (26-in.) mean diameter turbine was determined experimentally. The turbine was designed with a velocity diagram and physical features that were selected to be typical of a turbine for high-temperature-engine application. These characterizing features are thick blade profiles, blunt leading and trailing edges, and low solidity.

At equivalent design speed the two-stage turbine produced equivalent design specific work output with an efficiency of 0.932. This value compares closely with 0.929, which would be projected from the first-stage efficiency and the reheat effect. The mass flow rate for the two-stage turbine at these conditions was 1.015 design as compared with a corresponding mass flow rate obtained for the first stage of 1.018. Thus the mass-flow characteristics for the two stages were closely matched at design speed and specific-work output. The stage work-split at design equivalent operating conditions (speed and specific-work output) was 0.505-0.495, which was close to the design work split of 0.515-0.485.

The average turbine outlet flow angle at equivalent design speed and equivalent design specific work output was -5°, which is about 5° of underturning compared with the design velocity diagram. This result combined with the mass-flow rate (1.015 design) indicated that a small degree of overexpansion occurred in the second-stage stator and reduced reaction resulted in the second-stage rotor, both due to slightly oversizing the rotor outlet area.

INTRODUCTION

Many of the new engines designed in recent years for aircraft propulsion are using higher cycle temperatures to attain improved performance goals. The use of these

higher cycle temperatures necessitates cooling the turbine blades. This, in turn, dictates that the blading must be thick and have blunt leading and trailing edges to accommodate the internal coolant passages. The blade forms are, therefore, compromised from what would be considered optimum from an aerodynamic standpoint. The investigation of this type of turbine has been a part of the turbine research program at the NASA Lewis Research Center in the past few years. Two principal objectives of the investigation have been to determine the efficiency of the turbine with blading geometry compromised by cooling requirements and to determine the aerodynamic effect on performance of the coolant discharging into the turbine gas stream.

The turbine model used in this investigation was patterned after a two-stage turbine for a high-temperature-engine application. The cold-air model had a 66.04-centimeter (26-in.) mean diameter and a 10.16-centimeter (4-in.) blade height in the first stage. The design of the first stage is described in reference 1. The overall and detailed stator performance obtained with plain stator blading are given in references 1 and 2, respectively. Reference 3 presents the basic performance of the first stage obtained with plain blading. The effect of stator coolant air being discharged into the turbine gas stream on the performance of the first stage is described in references 4 to 6. In these tests the same basic stator design (ref. 1) was used, however, the blading was modified to incorporate the coolant flow. These tests provide an experimental measure of the aerodynamic effect of coolant addition and provide coefficients for analytical procedures such as references 7 and 8. The inclusion of the second stage is required to determine the effect of coolant ejected from the second-stage stator blade row. It is also of interest to determine the effect of coolant admitted from the first-stage blade rows on the performance of the two-stage configuration.

This report presents the design of the second stage and the performance results obtained with the two-stage turbine. The performance results were obtained with plain blading to establish a basis for comparison with follow-on tests which will include coolant addition in the various blade rows. In addition to the overall performance the results include turbine outlet flow angle, stage work-split at design speed, and second-stage stator mean section velocity distribution at approximately design conditions. The turbine inlet conditions were 1.0159×10^5 newtons per square meter (2121.8 lb/ft^2) and 378 K (680° R). The turbine was operated over a range of speeds from 40 to 108 percent design speed and over a range of total pressure ratios from 1.4 to 4.0.

SYMBOLS

A area, m^2; ft^2

g force-mass conversion constant, unity in SI system; 32.174 ft/sec^2

h specific enthalpy, J/kg; Btu/lb

N rotational speed, rpm

p absolute pressure, N/m^2; lb/ft^2

R gas constant for the mixture of air and combustion products used herein, 288 J/(kg)(K); 53.527 (ft-lb)/(lb)(^oR)

T temperature, K; ^oR

U blade velocity, m/sec; ft/sec

V absolute gas velocity, m/sec; ft/sec

W gas velocity relative to rotor blade, m/sec; ft/sec

w mass-flow rate (consists of sum of air flow and fuel flow), kg/sec; lb/sec

α absolute gas flow angle measured from axial direction, deg

$\overline{\alpha}$ average absolute gas flow angle at turbine outlet measured as average deviation from axial direction used in eq. (2), deg

β relative gas flow angle measured from axial direction

γ ratio of specific heats, 1.398 for the mixture of air and combustion products used herein

δ ratio of inlet pressure to U.S. standard sea-level pressure

ϵ function of γ, $\frac{0.73959}{\gamma}\left[\left(\frac{\gamma+1}{\gamma}\right)^{\gamma/\gamma-1}\right]$

η efficiency based on total pressure ratio

θ_{cr} squared ratio of critical velocity at turbine inlet to critical velocity of U.S. standard sea-level air

τ torque, N-m (ft-lb)

Subscripts:

cr condition at Mach 1

h turbine blade hub section

m turbine blade mean section

t turbine blade tip section

u tangential component

x axial component

0 station at turbine inlet, see fig. 6

1 station at first-stage stator outlet

2 station at first-stage rotor outlet

3 station at second-stage stator outlet

4 station at second-stage rotor outlet

Superscript:

' total state

SECOND STAGE BLADE DESIGN

The design requirements and physical features of the first stage were described in references 1 and 3. The second stage was specified to have the same mean diameter (0.6604 m; 26 in.), an average outlet flow angle of -10°, and a specific work output of 37 245 joules per kilogram (16.00 Btu/lb). Thus the design requirements for the two-stage turbine are as follows:

Equivalent specific work output, $\Delta h/\theta_{cr}$, J/kg; Btu/lb	76 818; 33.00
Equivalent mean blade speed, $U_m/\sqrt{\theta_{cr}}$, m/sec; ft/sec	152.4; 500.00
Equivalent mass flow, $(\epsilon w \sqrt{\theta_{cr}})/\delta$, kg/sec; lb/sec	18.1; 39.9

From these the following operating parameters are derived:

Equivalent design speed, $N/\sqrt{\theta_{cr}}$, rpm	4407.36
Equivalent design torque, $\epsilon\tau/\delta$, N-m; ft-lb	3009.88; 2219.97
Equivalent design mass flow-speed parameter, $\epsilon wN/\delta$, (kg)(rpm)/sec; (lb)(rpm)/sec	79 764; 175 854

A second-stage velocity diagram was evolved to conform to these requirements. The actual outlet total state of the first stage from reference 3 was used for the second-stage inlet total-state conditions. A stage efficiency of 0.88 was used to obtain the second-stage rotor outlet total-state conditions and a stator loss total pressure ratio of 0.97 was used to determine stator outlet total state conditions. The resulting velocity diagram for the second stage is shown in figure 1, and the velocity values are listed in table I. The velocity diagram of the first stage (from ref. 1) is included in the figure. The velocity diagram for the second stage is quite similar to the first-stage diagram. This would be expected since the mean blade speeds are the same and the specific work output of the second stage is 0.94 that of the first stage. The average stage loading

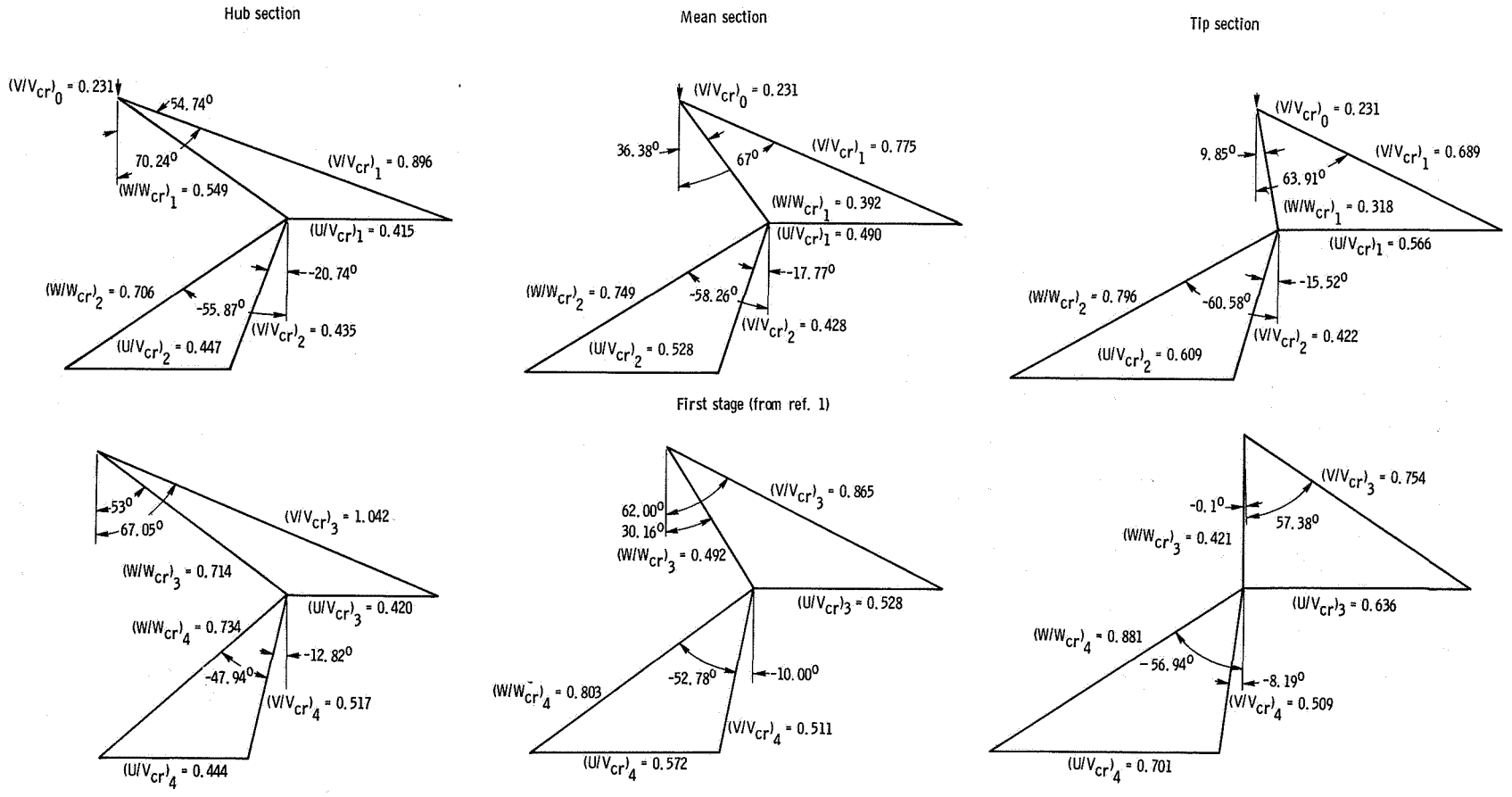

Figure 1. - Turbine design velocity diagram.

TABLE I. - VELOCITY DIAGRAM VECTOR VALUES

[All velocities in m/sec (ft/sec) based on turbine inlet conditions of U.S. standard sea level air.]

	Hub	Mean	Tip
	First stage		
U_1, U_2	129.0 (423.1)	152.4 (500)	175.8 (576.9)
$V_{u,1}$	262.1 (859.8)	221.8 (727.6)	192.2 (630.5)
$V_{u,2}$	44.5 (146.1)	37.7 (123.6)	32.7 (107.2)
$V_{x,1}$	94.1 (308.8)	94.1 (308.8)	94.1 (308.8)
$V_{x,2}$	117.6 (385.8)	117.6 (385.8)	117.6 (385.8)
V_1	278.5 (913.6)	240.9 (790.4)	214.0 (702.1)
V_2	125.7 (412.5)	123.5 (405.1)	122.0 (400.4)
W_1	163.0 (534.9)	116.9 (383.6)	95.5 (313.4)
W_2	209.6 (687.6)	223.5 (733.3)	239.4 (785.4)
	Second stage		
U_3	121.3 (398.1)	152.4 (500)	183.4 (601.9)
U_4	118.1 (387.5)	152.4 (500)	186.7 (612.5)
$V_{u,3}$	277.0 (908.8)	220.6 (723.6)	183.2 (601.1)
$V_{u,4}$	30.5 (100.1)	23.6 (77.6)	19.3 (63.3)
$V_{x,3}$	117.3 (384.7)	117.3 (384.7)	117.3 (384.7)
$V_{x,4}$	134.1 (440.0)	134.1 (440.0)	134.1 (440.0)
V_3	300.8 (986.8)	249.8 (819.5)	217.5 (713.7)
V_4	137.5 (451.2)	136.2 (446.8)	135.5 (444.5)
W_3	194.9 (639.4)	135.6 (445.0)	117.3 (384.7)
W_4	200.2 (656.8)	221.3 (726.1)	245.8 (806.5)

factor $(\Delta V_u/U)_m$ was 1.7 and 1.6 for the first and second stages, respectively. In general, both stages have conservative velocity diagrams (low stage loading factor) with no particular problems of high Mach number or excessive turning, and a high performance level would be anticipated.

The axial velocities at the second-stage stator outlet and rotor outlet were increased compared with their counterparts in the first stage by 25 percent and 14 percent, respectively. With this increase in axial velocity level an increase in annulus area was still required in both of the second-stage blade rows. The blade height was 13.46 centimeters (5.298 in.) at the stator outlet and 14.86 centimeters (5.852 in.) at the rotor outlet. The manner of providing the flow area is shown in the flow path projection in figure 2. In general, the walls were flared out at a cone angle to attain a constant diam-

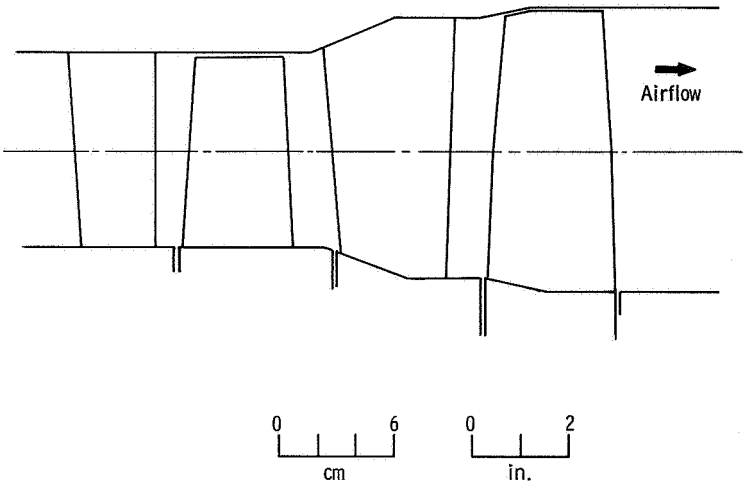

Figure 2. - Projection of flow path in radial-axial plane for two-stage cold air turbine.

eter section (the diameters being those of the blade outlet) well ahead of the blade channel outlet orthogonal.

The physical features of the second stage duplicated those of the first stage unless other considerations dictated otherwise. The number of blades comprising the two second-stage blade rows was selected to increase the blade loading somewhat from that used in the first stage. The second-stage stator consisted of 39 blades, and the rotor contained 52. The resulting Zweifel loading factors (ref. 9) were 0.85 and 0.91 for the stator blade and rotor blade, respectively. The corresponding loading factors for the first stage were 0.68 and 0.84 for the stator and rotor, respectively. Curved back suction surfaces were used at the blade inlets and outlets as discussed in reference 1. The trailing-edge radius of both blade rows was 0.089 centimeter (0.035 in.), the same as the first-stage blading. The second-stage stator blade employed the same leading-edge radius of 0.381 centimeter (0.150 in.) that was used in the first-stage blade rows. This leading-edge radius, however, would have caused a severe area contraction at the hub section of the second-stage rotor blade. Therefore, the leading-edge radius for this blade row was varied with blade height, being 0.127 centimeter (0.050 in.) at the hub section, 0.254 centimeter (0.100 in.) at the mean section, and 0.381 centimeter (0.150 in.) at the tip section.

The blade channel design procedure is quasi-three dimensional and is described in reference 1. The same basic assumptions that were used in reference 1 for the first stage were applied to the design of the second stage blade-rows, namely, (1) free-vortex flow occurred at the free-stream stations between blade rows, (2) simple radial equilibrium was maintained throughout, and (3) the total pressure loss in the blade row varies linearly with length of mean flow path. The geometry of both second-stage blade rows was based on sectional layouts at the hub, mean, and tip radii. The hub and tip sections

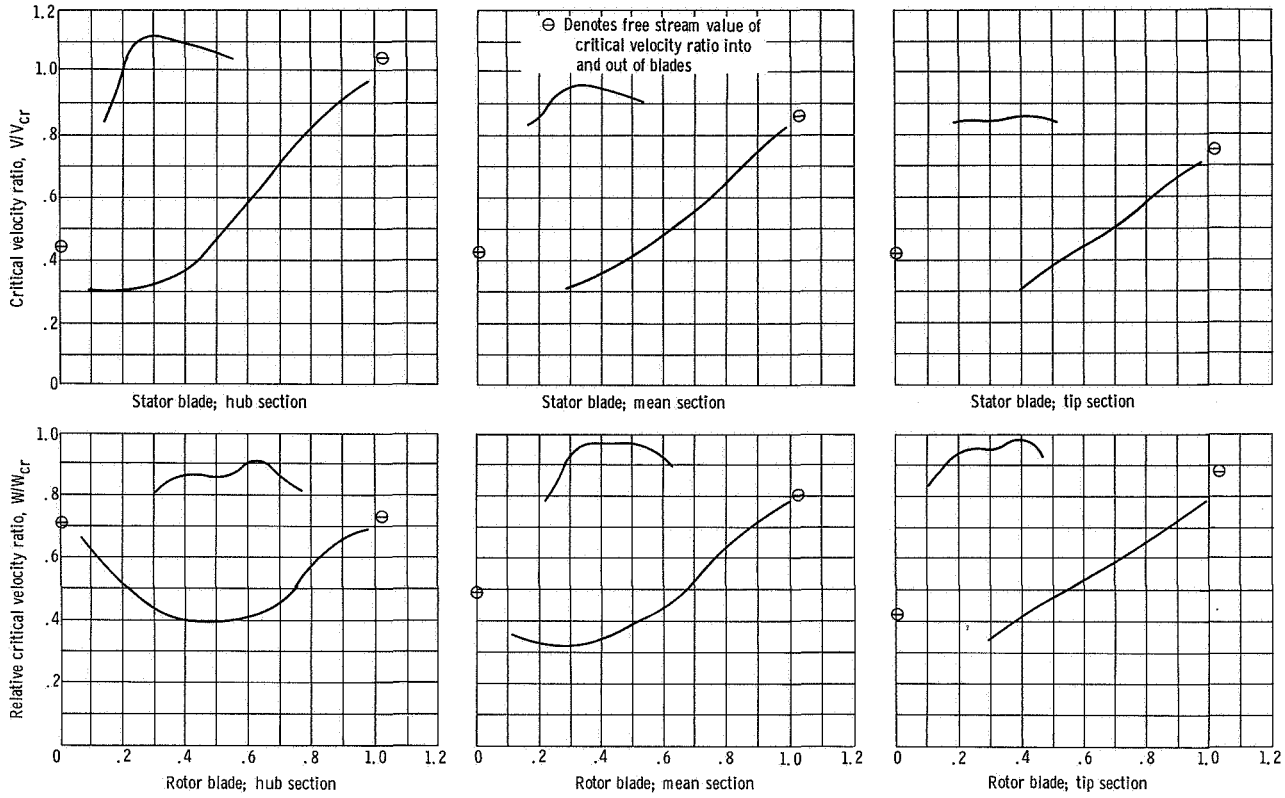

(a) Second stage.

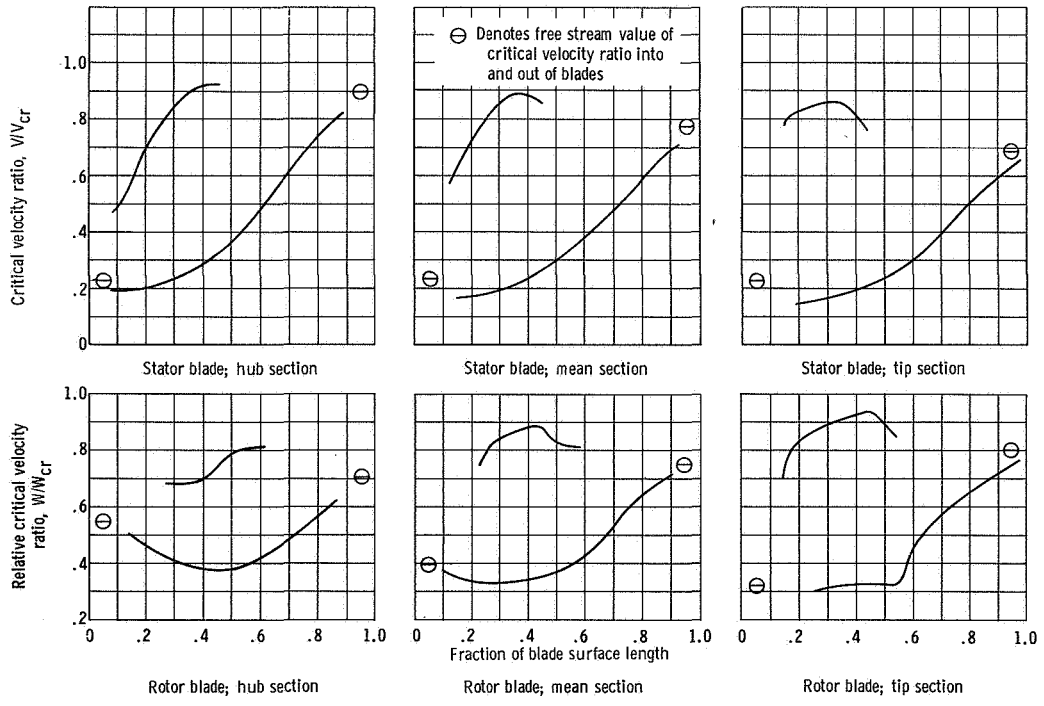

(b) First stage.

Figure 3. - Design blade-surface velocity distributions.

of both blade rows were taken at the greatest blade length corresponding to their radii at their outlet station (fig. 2). However, in the weight flow integration (eq. (4), ref. 1) used in the design procedure the actual blade hub and tip radii were used as the radial integration limits. The blade surface velocity distributions for the second stage are shown in figure 3. Those of the first-stage (ref. 1) are included in the figure for comparison. A similarity in the blade surface velocity distributions of the two stages can be noted. The higher blade loading employed in the design of the second-stage blade rows is evidenced by the greater spread between suction and pressure surface velocities. A sketch of the blade passages and profiles is shown in figure 4 for the two-stage turbine. The blading coordinates are listed in table II. A photograph of the two-stage rotor assembly is shown in figure 5.

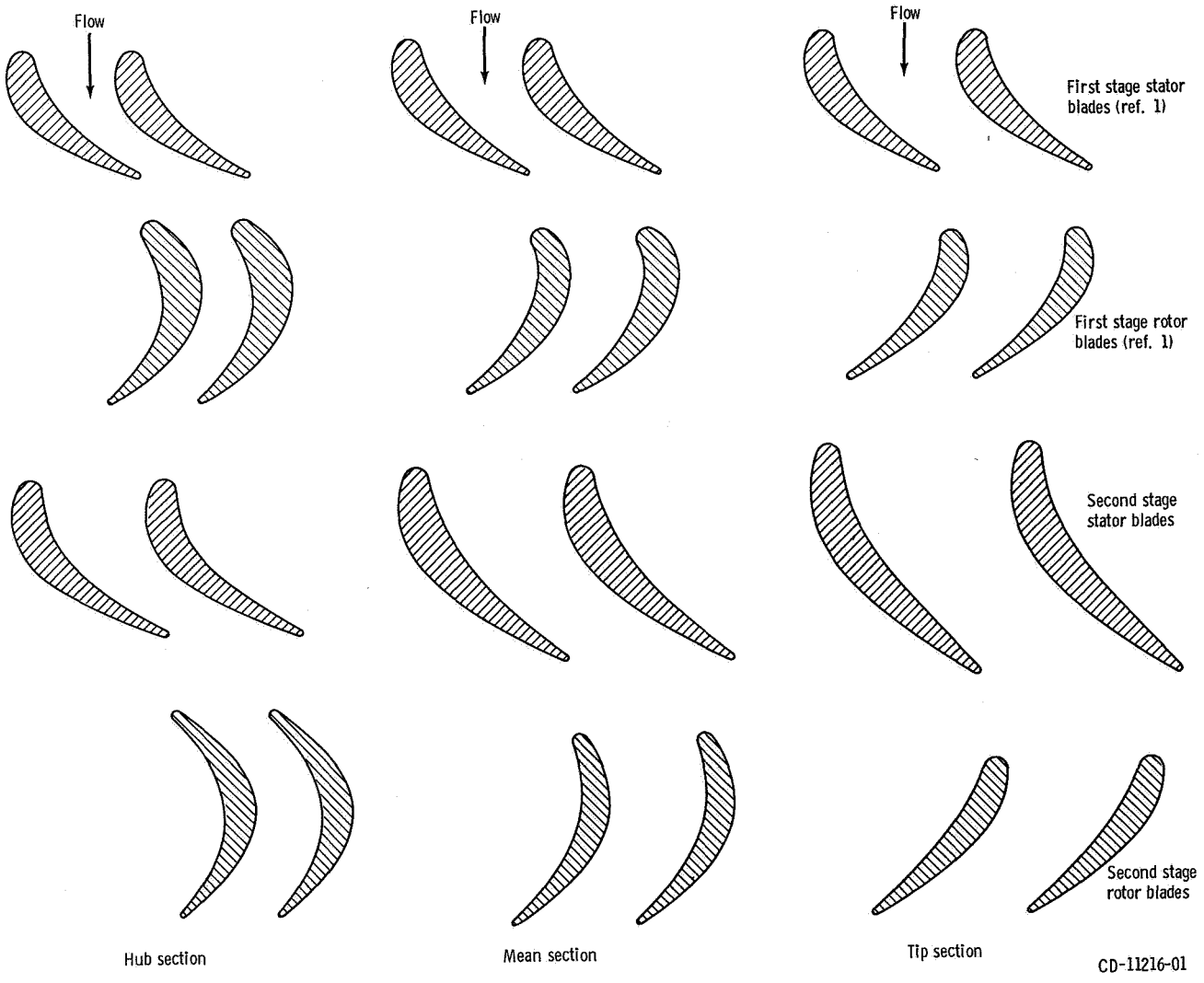

Figure 4. - Sketch of stator and rotor blade profiles and flow passages.

TABLE II. - TURBINE BLADE COORDINATES

(a) First-stage stator[a]

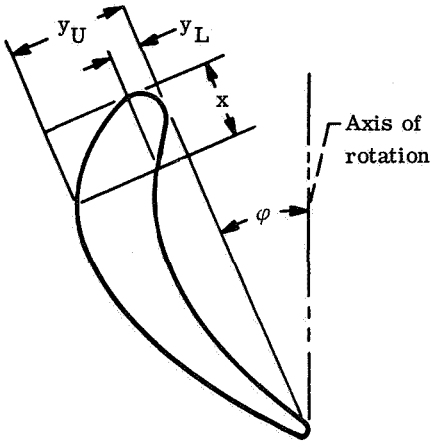

x, in.	Hub		Mean		Tip	
	Orientation angle, φ, deg					
	42.42		41.03		39.67	
	y_L, in.	y_U, in.	y_L, in.	y_U, in.	y_L, in.	y_U, in.
0	0.150	0.150	0.150	0.150	0.150	0.150
.100	-----	.375	-----	.394	-----	.427
.200	-----	.486	-----	.514	-----	.550
.300	.060	.558	.061	.588	.063	.621
.400	.105	.603	.106	.636	.111	.665
.500	.143	.630	.145	.665	.148	.688
.600	.174	.643	.174	.676	.179	.696
.700	.197	.643	.196	.675	.203	.690
.800	.214	.635	.210	.663	.217	.675
.900	.226	.618	.219	.644	.227	.651
1.000	.230	.595	.223	.619	.231	.625
1.100	.228	.570	.221	.590	.229	.597
1.200	.223	.541	.215	.560	.223	.565
1.300	.212	.508	.205	.527	.214	.535
1.400	.196	.473	.191	.492	.200	.500
1.500	.175	.433	.175	.452	.183	.462
1.600	.153	.391	.155	.410	.163	.422
1.700	.128	.345	.133	.365	.140	.380
1.800	.103	.295	.111	.319	.117	.335
1.900	.075	.242	.086	.267	.095	.287
2.000	.046	.183	.060	.214	.070	.237
2.100	.016	.121	.033	.157	.045	.185
2.197	.035	-----	-----	-----	-----	-----
2.200	-----	-----	.005	.096	.021	.130
2.263	-----	-----	.035	.035	-----	-----
2.327	-----	-----	-----	-----	.035	.035

[a]From ref. 1.

TABLE II. - Continued. TURBINE BLADE COORDINATES

(b) First-stage rotor[a]

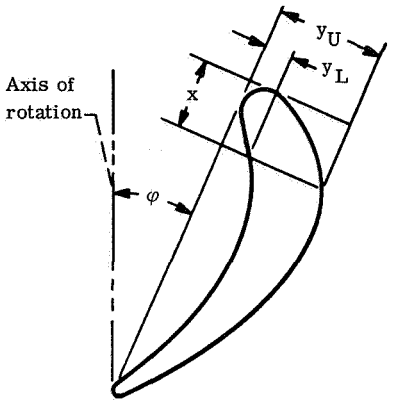

x, in.	Hub		Mean		Tip	
	Orientation angle, φ, deg					
	11.31		22.87		34.67	
	y_L, in.	y_U, in.	y_L, in.	y_U, in.	y_L, in.	y_U, in.
0	0.150	0.150	0.150	0.150	0.150	0.150
.100	-----	.393	-----	.358	-----	.312
.200	-----	.536	-----	.490	-----	.397
.300	.075	.642	.078	.593	.066	.468
.400	.149	.725	.153	.668	.122	.523
.500	.219	.788	.217	.722	.168	.565
.600	.283	.839	.267	.755	.204	.593
.700	.338	.875	.307	.774	.232	.610
.800	.383	.900	.339	.781	.250	.614
.900	.416	.913	.360	.775	.262	.609
1.000	.439	.913	.373	.759	.264	.594
1.100	.453	.902	.377	.734	.261	.573
1.200	.458	.878	.373	.702	.252	.547
1.300	.454	.845	.362	.664	.237	.519
1.400	.442	.801	.342	.620	.220	.487
1.500	.422	.748	.315	.573	.200	.453
1.600	.393	.689	.283	.523	.177	.416
1.700	.356	.624	.244	.466	.153	.377
1.800	.312	.555	.203	.407	.128	.333
1.900	.260	.481	.159	.346	.103	.288
2.000	.202	.400	.113	.277	.077	.238
2.100	.140	.312	.067	.204	.050	.185
2.200	.072	.216	.022	.125	.022	.128
2.290	-----	-----	.035	.035	-----	-----
2.300	-----	.110	-----	-----	-----	-----
2.321	-----	-----	-----	-----	.035	.035
2.354	.035	.035	-----	-----	-----	-----
	Stacking axis coordinates					
	x = 1.200	y = 0.401	x = 1.110	y = 0.376	x = 1.080	y = 0.337

[a]From ref. 1.

TABLE II. - Continued. TURBINE BLADE COORDINATES

(c) Second stage stator

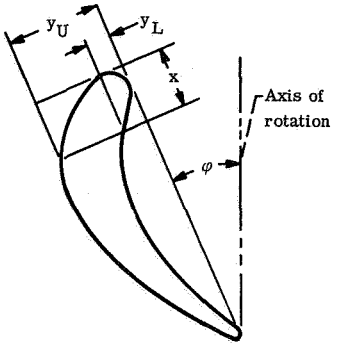

x, in.	Hub		Mean		Tip	
	Orientation angle, φ, deg					
	40.06		37.11		34.96	
	y_U, in.	y_L, in.	y_U, in.	y_L, in.	y_U, in.	y_L, in.
0	0.150	0.150	0.150	0.150	0.150	0.150
.100	.368	-----	.343	-----	.316	-----
.200	.501	-----	.458	-----	.417	-----
.300	.596	.070	.549	.057	.507	.061
.400	.663	.154	.622	.102	.583	.112
.500	.710	.213	.677	.139	.648	.157
.600	.740	.261	.719	.173	.700	.197
.700	.757	.299	.749	.201	.740	.232
.800	.762	.326	.767	.225	.770	.260
.900	.756	.346	.776	.244	.793	.283
1.000	.743	.360	.778	.258	.805	.299
1.100	.723	.364	.772	.268	.812	.309
1.200	.696	.363	.761	.275	.813	.314
1.300	.666	.355	.745	.278	.808	.313
1.400	.632	.342	.725	.278	.798	.311
1.500	.597	.323	.701	.276	.784	.303
1.600	.559	.302	.676	.272	.767	.294
1.700	.521	.277	.650	.264	.746	.282
1.800	.480	.250	.622	.255	.724	.268
1.900	.437	.222	.590	.243	.700	.254
2.000	.393	.192	.558	.229	.674	.241
2.100	.346	.162	.524	.214	.647	.226
2.200	.298	.131	.487	.197	.617	.212
2.300	.248	.099	.447	.179	.585	.196
2.400	.196	.068	.407	.158	.552	.181
2.500	.141	.036	.364	.137	.515	.165
2.600	.085	-----	.317	.114	.477	.149
2.653	.035	.035	-----	-----	-----	-----
2.700	-----	-----	.270	.090	.437	.132
2.800	-----	-----	.218	.064	.395	.115
2.900	-----	-----	.165	.039	.350	.097
3.000	-----	-----	.109	.013	.302	.079
3.093	-----	-----	.035	.035	-----	-----
3.100	-----	-----	-----	-----	.253	.060
3.200	-----	-----	-----	-----	.199	.041
3.300	-----	-----	-----	-----	.144	.022
3.400	-----	-----	-----	-----	.086	-----
3.455	-----	-----	-----	-----	.035	.035
	Stacking axis coordinates					
	x = 0.518	y = 0.420	x = 0.864	y = 0.441	x = 1.193	y = -0.489

TABLE II. - Concluded. TURBINE BLADE COORDINATES

(d) Second stage rotor

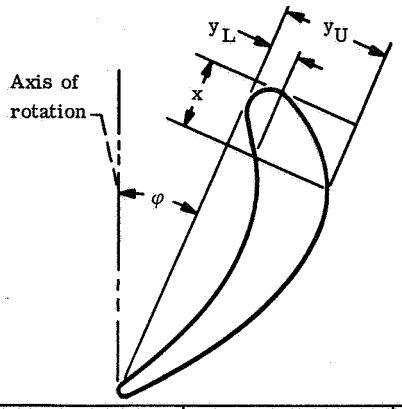

x, in.	Hub		Mean		Tip	
	Orientation angle, φ, deg					
	-2.86		19.06		38.02	
	y_U, in.	y_L, in.	y_U, in.	y_L, in.	y_U, in.	y_L, in.
0	0.050	0.050	0.100	0.100	0.150	0.150
.100	.203	.025	.259	-----	.301	-----
.200	.326	.109	.370	.052	.366	-----
.300	.437	.191	.466	.127	.418	.043
.400	.540	.268	.553	.193	.457	.074
.500	.634	.339	.625	.249	.485	.100
.600	.720	.402	.683	.296	.503	.119
.700	.797	.455	.723	.335	.513	.134
.800	.865	.500	.751	.365	.515	.143
.900	.918	.537	.767	.387	.511	.146
1.000	.959	.566	.773	.403	.501	.146
1.100	.986	.587	.769	.410	.486	.142
1.200	1.001	.603	.757	.412	.470	.137
1.300	1.003	.609	.737	.406	.452	.131
1.400	.992	.610	.708	.394	.431	.124
1.500	.972	.603	.673	.378	.407	.117
1.600	.939	.586	.634	.355	.383	.108
1.700	.896	.562	.588	.327	.356	.099
1.800	.841	.527	.540	.295	.327	.089
1.900	.773	.483	.487	.259	.295	.078
2.000	.695	.427	.431	.221	.261	.066
2.100	.609	.365	.373	.180	.224	.053
2.200	.516	.294	.309	.137	.186	.039
2.300	.415	.215	.242	.093	.145	.025
2.400	.305	.133	.172	.048	.103	.010
2.496	-----	-----	-----	-----	.035	.035
2.500	.184	.047	.094	-----	-----	-----
2.554	-----	-----	.035	.035	-----	-----
2.602	.035	.035	-----	-----	-----	-----
	Stacking axis coordinates					
	x = 1.276	y = 0.559	x = 1.110	y = 0.389	x = 1.073	y = 0.213

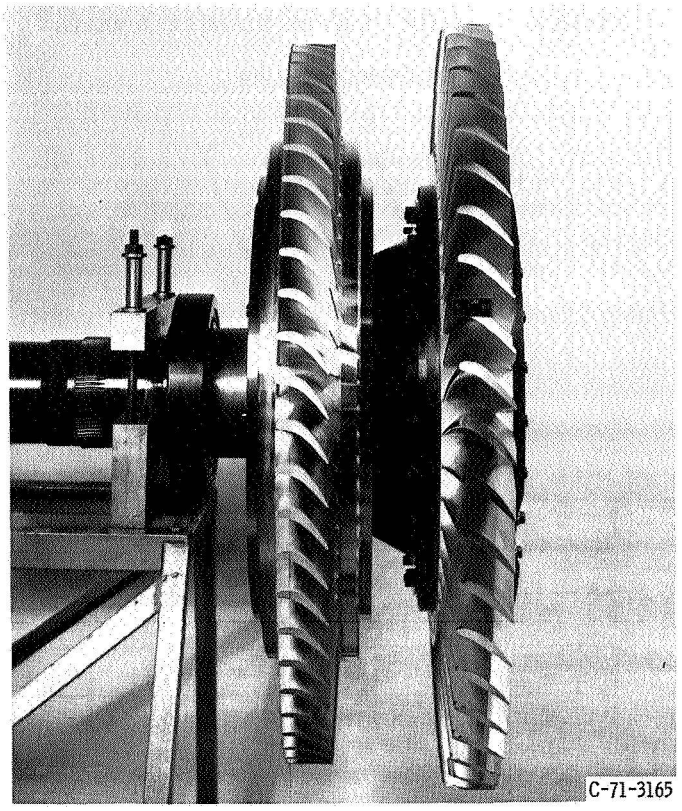

Figure 5. - Two-stage rotor assembly.

APPARATUS INSTRUMENTATION AND PROCEDURE

The test facility was that described in references 1 and 4 to 6, except for the modifications to accommodate the second stage. These modifications were redesigned turbine outlet casing and inner fairing pieces, the addition of a second dynamometer, and the addition of an inlet air heater. A second dynamometer was added because of the increased turbine torque output. The two units were operated in tandem with their stators tied together, thus the total stator reaction torque was indicated as one quantity. The inlet air heater was a vitiating type that used natural gas fuel. The purpose of the heater was to elevate the inlet temperature and avoid low-temperature problems at the turbine outlet. A sketch of the turbine test section is shown in figure 6.

The key research data and methods of acquiring the data are the same as described in the reference single-stage investigations and are reviewed briefly herein. Air flow was measured using a calibrated Dall tube, which is a special type of venturi meter. Fuel flow to the inlet air heater was measured using a flat-plate orifice. The turbine mass flow rate consisted of the sum of these two flows. Turbine rotative speed was measured with an electronic speed counter that registered the impulses as the teeth of

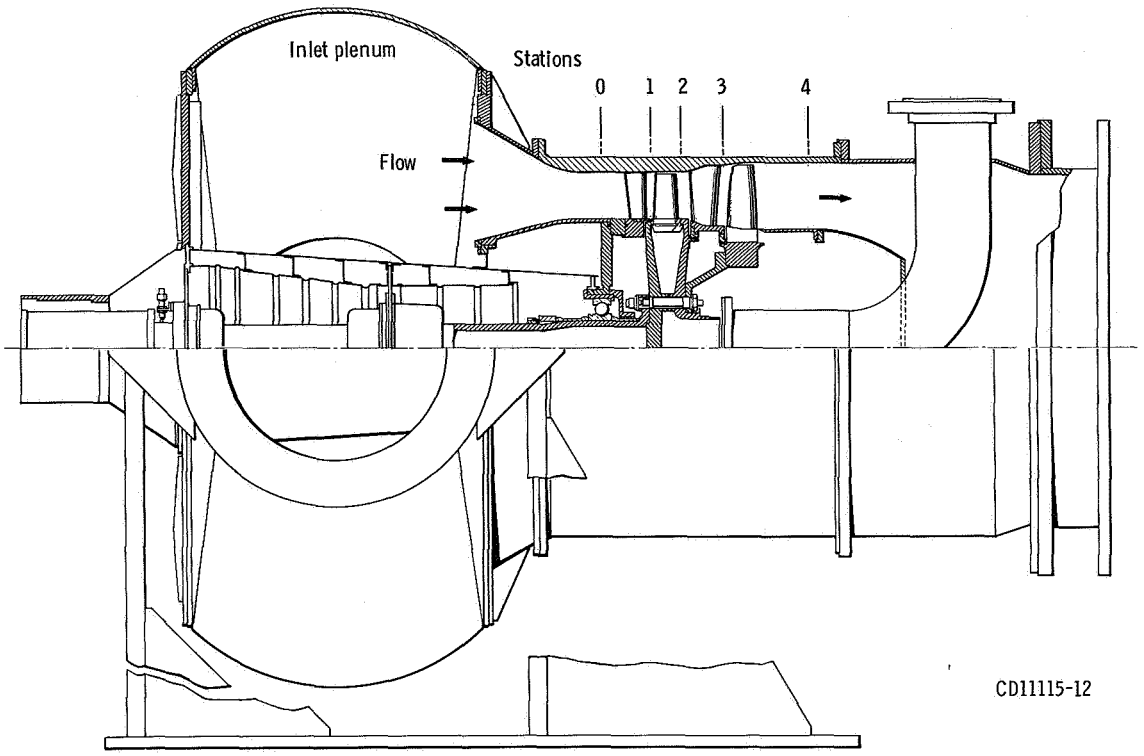

Figure 6. - Turbine test section.

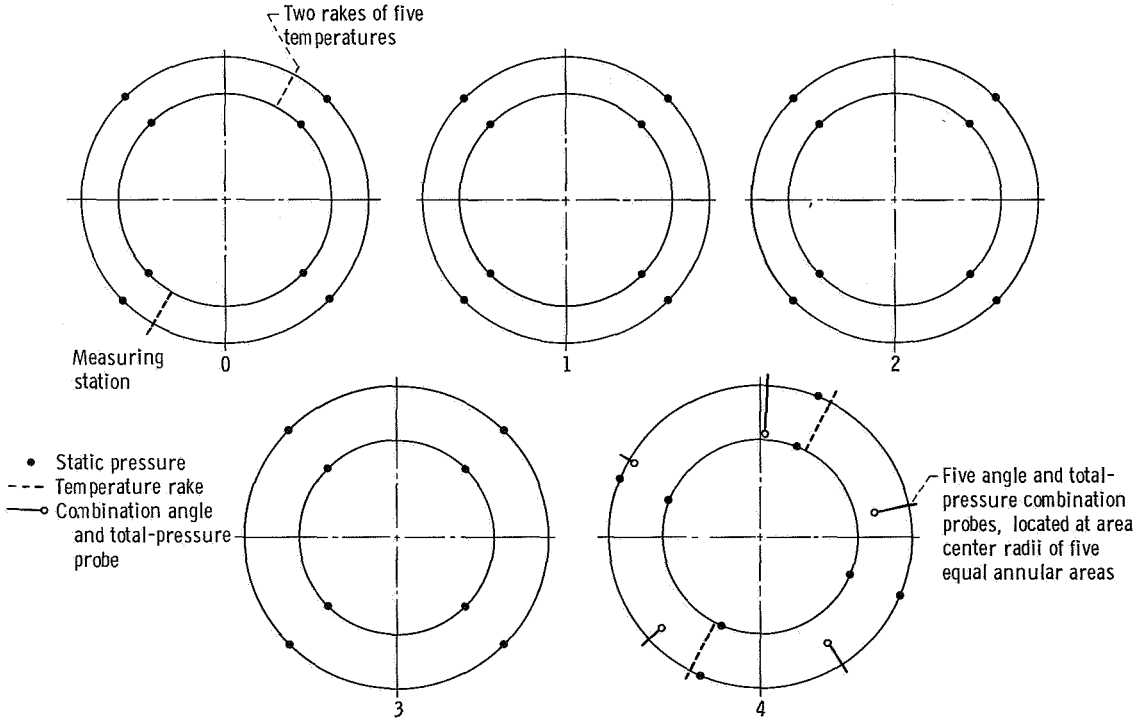

Figure 7. - Turbine instrumentation (looking upstream).

a sprocket on the turbine shaft passed by a fixed magnetic pickup mounted in close proximity thereto. The research and pressure and temperature measurements taken at the turbine test section are shown in the instrumentation plan figure 7.

In addition to the overall performance instrumentation, 30 static pressure taps were installed around the periphery of the second-stage stator blade at the mean radius. The blade surface static pressures were recorded for the operating conditions of design speed and approximately design equivalent specific work output.

The turbine was operated at inlet conditions of 1.0159×10^5 newtons per square meter (2121.8 lb/ft^2) and 378 K (680° R). A series of nine turbine speeds from 40 to 108 percent of design value were investigated. The speed was limited to 108 percent design because of vibration. At each speed the total-pressure ratio across the turbine was varied from about 1.4 to 4.0. Turbine inlet static pressure p_0, outlet static pressure p_4, and the surface pressures at the mean radius of the second stage stator were recorded by photographing a mercury manometer board. All other data information was obtained as an electrical signal from an appropriate transducer, which was transmitted to a 100-channel data recording system. The method of calculating inlet and outlet total pressures was the same as used in the reference investigations and is included for convenience. Inlet total pressure was calculated from static pressure, mass flow rate, and inlet total temperature using the following equation:

$$\frac{p'_0}{p_0} = \left[\frac{1}{2} + \sqrt{\frac{1}{4} + \frac{\gamma - 1}{2g\gamma}\left(\frac{w}{p_0 A_0}\right)^2 RT'_0}\right]^{\gamma/(\gamma-1)} \tag{1}$$

The equation for the outlet total pressure is of the same form except that allowance is made for the flow being at some angle to the axial direction.

$$\frac{p'_4}{p_4} = \left[\frac{1}{2} + \sqrt{\frac{1}{4} + \frac{\gamma - 1}{2g\gamma}\left(\frac{w}{p_4 A_4}\right)^2 \frac{RT'_4}{\cos^2\bar{\alpha}}}\right]^{\gamma/(\gamma-1)} \tag{2}$$

The total temperature T'_4 in equation (2) was derived from inlet total temperature, turbine speed, turbine torque output, and mass flow. The angle $\bar{\alpha}$ in equation (2) is the average deviation from the axial direction, irrespective of sign.

The performance data are shown as an overall performance map which was con-

structed in the following manner. The reduced data were first plotted on two primary result curves. The first plot was equivalent torque against total-pressure ratio, and the second, equivalent mass flow against total-pressure ratio. Smooth curves were then faired on these plots through the data points for each speed. Values of equivalent torque and equivalent mass flow were then obtained from these faired curves at various total pressure ratios to construct the performance map.

RESULTS AND DISCUSSION

The results include the overall performance map, stage work split at design speed, turbine outlet flow angle and the second stage stator blade velocity distribution. These subjects will be discussed in this order in the following sections.

Overall Performance

The data are shown in figures 8 and 9 with equivalent torque $\epsilon\tau/\delta$ and equivalent mass flow $(\epsilon w\sqrt{\theta_{cr}})/\delta$ shown as functions of the total-pressure ratio p'_0/p_4. The figures are made dimensionless by normalizing with the design value of the appropriate parameter. The deviation of the data points from the faired value can be noted in the figures. In figure 8 the torque curves are seen to be separated by turbine speed. In figure 9, however, this separation is quite small and an expanded scale is required to show the speed effect on mass flow. Actually the scatter, or deviation from faired value, is within 1/2 percent on torque and close to 1/4 percent on mass flow. The maximum mass flow at design speed is seen in figure 9 to be 1.017 design. The maximum mass flow obtained for the first-stage configuration at design speed was 1.036 design (ref. 3). Thus, the second stage appears to have a slight limiting effect on choking mass flow.

The overall performance map is shown in figure 10 with equivalent specific work output $\Delta h/\theta_{cr}$ shown as a function of equivalent mass flow-speed parameter $(\epsilon wN)/\delta$ for the various speeds. Constant total-pressure lines and efficiency contours are superimposed on the figure. As noted for the first-stage configuration (ref. 3), the two-stage turbine had a fairly wide range of operating conditions at efficiencies of 0.85 or better. At design values of speed and specific work output the efficiency was 0.932. This is very close to an estimated two-stage efficiency 0.929, based on design work output in each stage and a stage efficiency of 0.923 for both stages. This efficiency, 0.923, was obtained in reference 3 for the first stage, and the difference between the 0.929 and 0.923 is due to the reheat effect. Thus the second stage performed as well or slightly better than that might be expected based on the first-stage performance. The highest

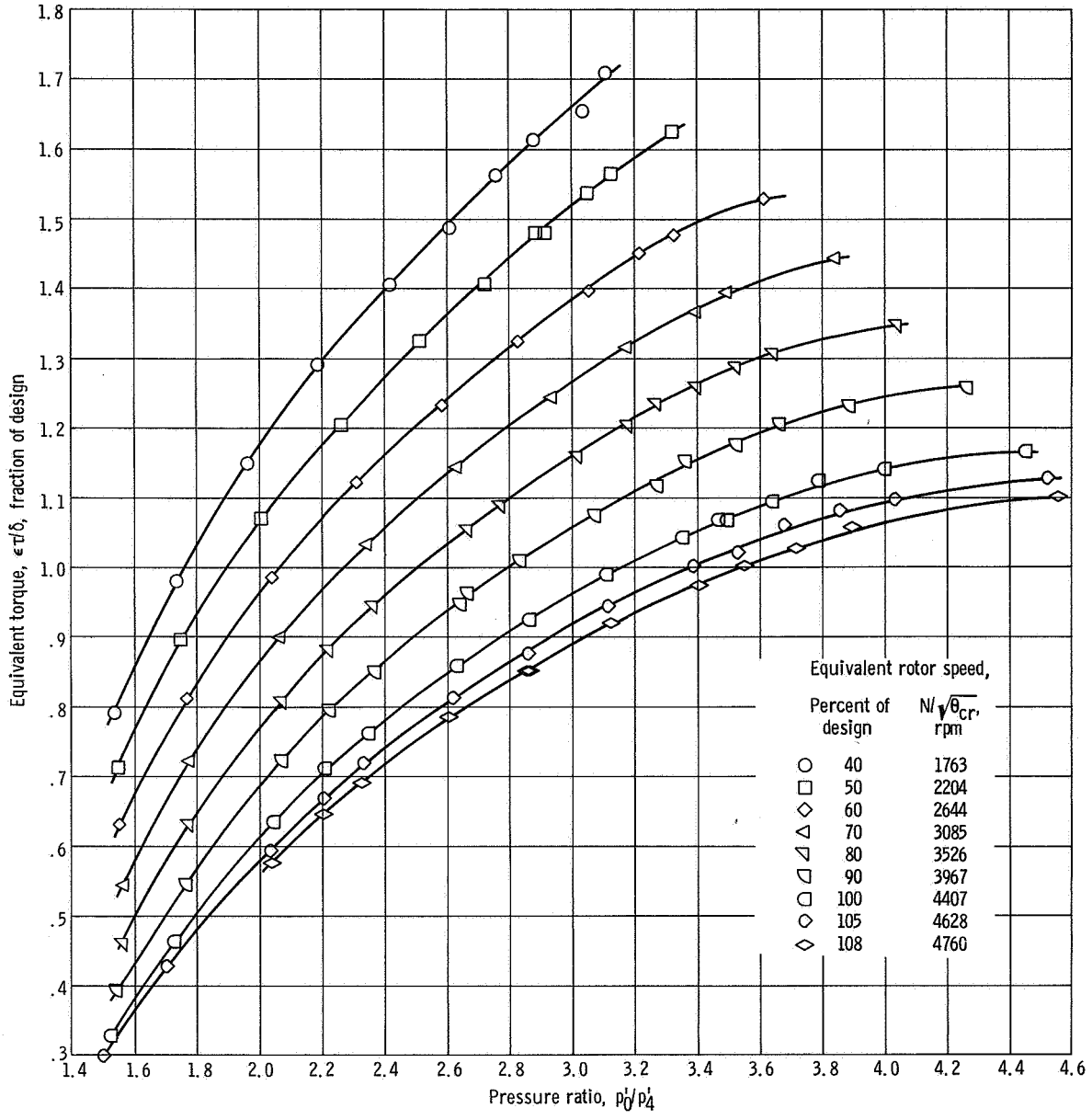

Figure 8. - Variation of equivalent torque with pressure ratio and equivalent speed.

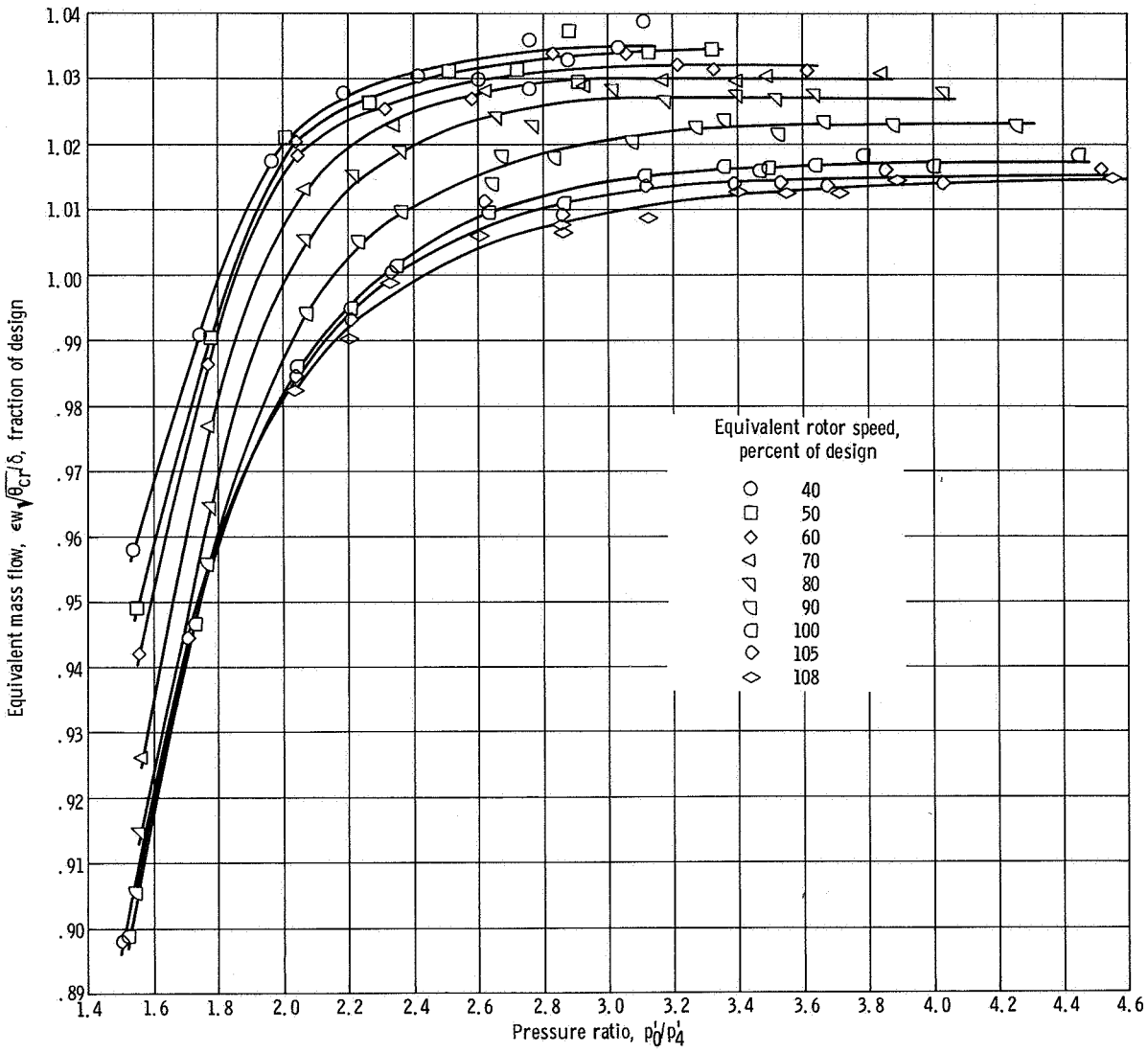

Figure 9. - Variation of equivalent mass flow with pressure ratio and equivalent speed.

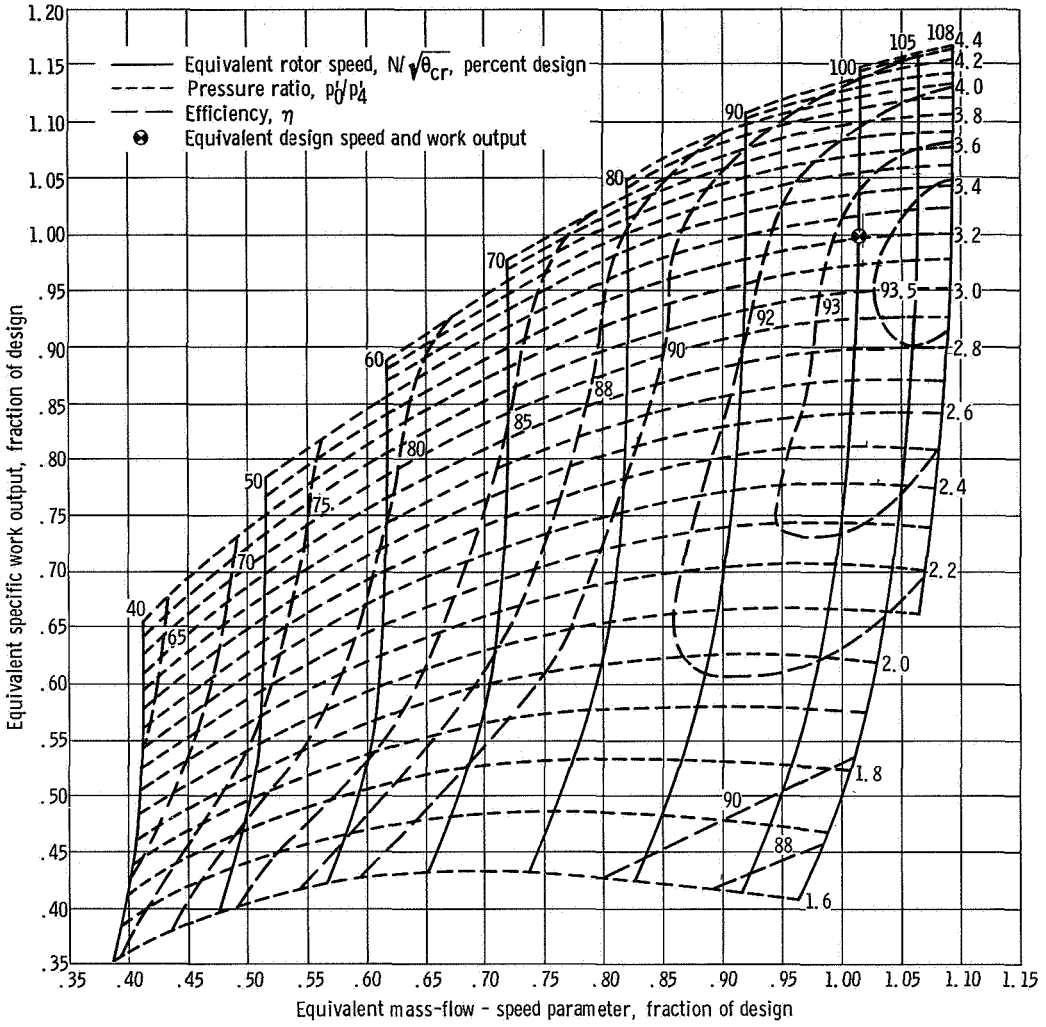

Figure 10. - Performance map. Design value of specific work output, 76 818 joules per kilogram; design value of mass-flow - speed parameter, 79 764 kilogram-rpm per second.

efficiency obtained for the two-stage configuration was 0.935 at 105 and 108 percent design speed.

The mass flow obtained at design speed and design specific work output is seen in figure 10 (by the abscissa scale) to be 1.015 design value. The corresponding value obtained for the first stage in reference 3 was 1.018. Thus the mass-flow characteristics of the two stages are closely matched at design speed and work output.

Stage Work Split

In figure 11 the distribution of specific work output between the two stages is shown for design speed over a range of pressure ratio by the lower curve. The upper curve in the figure is the fraction of design two-stage work output developed by both stages. The work output of the first stage was obtained from reference 3 by relating the first-stage work output to the equivalent mass flow, since both of these quantities were specified by the total-pressure ratio in the reference. The assumption was then made that for a given mass flow rate the first stage work output was the same as a part of the two-stage configuration as it was in the first-stage test (ref. 3). The fraction of total work developed by the first stage is seen to range from 0.648 to 0.454 as the total pressure ratio p'_0/p'_4 is varied from 2.0 to 4.0. At the pressure ratio of 3.215, corresponding to the two-stage design work output (upper curve), the first stage produced 0.505 of the

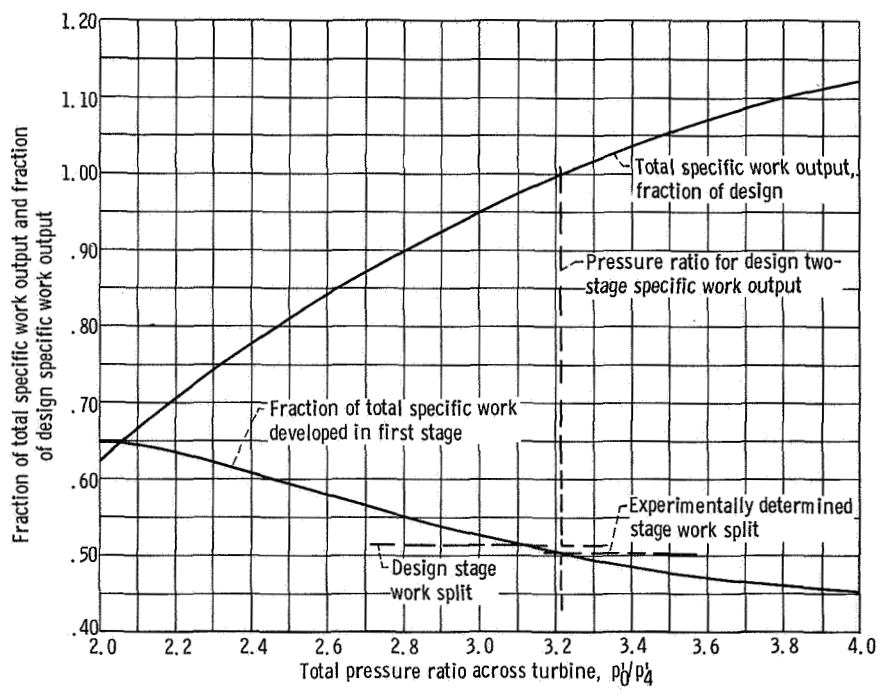

Figure 11. - Distribution of specific work output between the two stages at design speed.

total work output. Thus, the stage-work split obtained experimentally at design speed and design work was 0.505-0.495, which is close to the design work split of 0.515-0.485.

Turbine Outlet Flow Angle

The average turbine outlet flow angle is shown in figure 12 as a function of total pressure ratio for the various speeds. Each data point represents the algebraic average

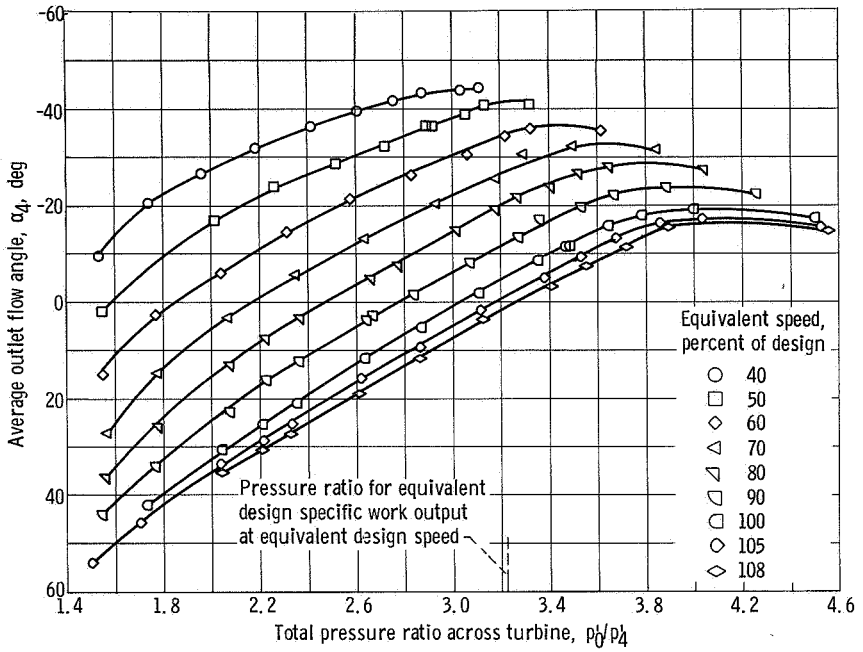

Figure 12. - Variation of average outlet flow angle with turbine total pressure ratio for various speeds.

of the 5 angle measurements that were made at station 4 at the area-center radii of 5 equal annular areas. The negative sign of the angle means that the flow is opposite in direction to the blade speed and the outlet swirl is a positive contribution to the work output. The trends of flow angle with pressure ratio are similar to those obtained with the first stage (refs. 3 and 4). At the condition of design equivalent specific work output at design speed, the flow angle was -5°. This angle can be compared with -10°, which would be obtained from the design velocity diagram. This slight underturning and the mass flow being 1.015 design value indicate that the flow overexpanded in the stator. As a result, a smaller outlet swirl contribution was required to produce design equivalent work, and the reaction in the rotor was less than design. This probably resulted (as discussed in ref. 3) from the use of a conservative estimate of stage efficiency, 0.88, which in turn caused the rotor outlet area to be slightly oversized.

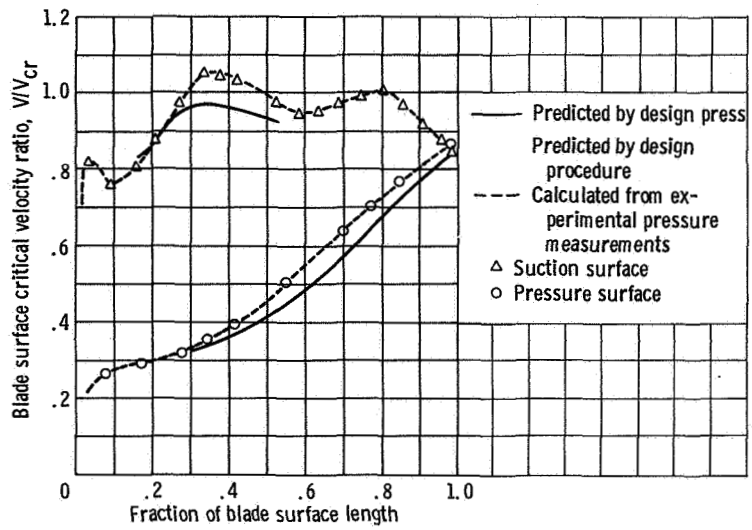

Figure 13. - Comparison of blade surface velocity distribution obtained from design procedure with that determined from experimental pressure measurements for second-stage stator blade mean section.

Stator Blade Velocity Distribution

The velocity distribution of the second-stage stator blade mean section determined from the static-pressure measurements is compared with that predicted from the design procedure in figure 13. The critical velocity ratio was obtained from the local static pressure using the isentropic relation

$$\frac{V}{V_{cr}} = \left\{ \frac{\gamma + 1}{\gamma - 1} \left[1 - \left(\frac{p}{p'} \right)^{\gamma - 1/\gamma} \right] \right\}^{1/2} \tag{3}$$

The total pressure was taken as the static pressure which was read from either of two taps located near the forward stagnation point. This calculated velocity distribution is shown as the dashed line passing through the data points in figure 13. The velocity distribution predicted by the design procedure is shown as the solid line in the figure and is very similar to that shown in figure 3. The reason for the slight difference between the velocity distributions shown in figures 3 and 13 is that the channel total pressure loss used in the design procedure (and reflected in fig. 3) has been factored out in figure 13 as discussed in reference 1.

The design procedure fairly accurately predicted the shape of the velocity distribution curve. The surface velocities based on experimental pressure measurements were in most cases slightly higher than the predicted values. A small hump occurred in the

suction surface velocity curve downstream of the throat. A similar effect was noted for the first-stage stator (ref. 1), although the reexpansion was less pronounced. The equivalent specific work output at this operating condition was 0.975 design value.

SUMMARY OF RESULTS

A two-stage turbine designed with physical features and a velocity diagram typical of those for a high-temperature-engine application has been investigated experimentally in cold air. The results include the overall performance, stage work split at design speed, turbine outlet flow angle variation, and second-stage stator velocity distribution. The pertinent results are summarized as follows:

1. The efficiency of the two-stage configuration was 0.932 at conditions of equivalent design speed and equivalent design specific work output. This compared favorably with the value of 0.929 estimated by assuming the first-stage efficiency for both stages and accounting for the reheat effect.

2. The mass flow of the two-stage turbine at equivalent design speed and equivalent design specific work output was 1.015 design, as compared with 1.018 design mass flow obtained for the first stage in a reference investigation. Thus, the mass flow characteristics of the two stages at design operating conditions were closely matched.

3. At equivalent design operating conditions (speed and specific work output) the stage work split was 0.505-0.495 which was close to the design work split of 0.515-0.485.

4. The average outlet flow angle at the equivalent design operating conditions (speed and specific work output) was -5° compared with the design value of -10°. This result together with the mass flow (1.015 design) indicate that overexpansion occurred in the second-stage stator and a reduced reaction occurred in the rotor as a result of slightly oversizing the rotor outlet area.

Lewis Research Center,
National Aeronautics and Space Administration,
Cleveland, Ohio, May 24, 1972,
764-74.

REFERENCES

1. Whitney, Warren J.; Szanca, Edward M.; Moffitt, Thomas P.; and Monroe, Daniel E.: Cold-Air Investigation of a Turbine for High-Temperature-Engine Application. I - Turbine Design and Overall Stator Performance. NASA TN D-3751, 1967.

2. Prust, Herman W., Jr.; Schum, Harold J.; and Behning, Frank P.: Cold-Air Investigation of a Turbine for High-Temperature Engine Application. II - Detailed Analytical and Experimental Investigation of Stator Performance. NASA TN D-4418, 1968.

3. Whitney, Warren J.; Szanca, Edward M.; Bider, Bernard; and Monroe, Daniel E.: Cold-Air Investigation of a Turbine for High-Temperature-Engine Application. III - Overall Stage Performance. NASA TN D-4389, 1968.

4. Szanca, Edward M.; Schum, Harold J.; and Prust, Herman W., Jr.: Cold-Air Investigation of a Turbine with Stator-Blade Trailing-Edge Coolant Ejection. III - Overall Stage Performance. NASA TM X-1974, 1970.

5. Szanca, Edward M.; Schum, Harold J.; and Behning, Frank P.: Cold-Air Investigation of a Turbine with Transpiration-Cooled Stator Blades. II - Stage Performance with Discrete Hole Stator Blades. NASA TM X-2133, 1970.

6. Behning, Frank P.; Schum, Harold J.; and Szanca, Edward M.: Cold-Air Investigation of a Turbine with Transpiration-Cooled Stator Blades. IV - Stage Performance with Wire-Mesh Shell Stator Blading. NASA TM X-2176, 1971.

7. Whitney, Warren J.: Analytical Investigation of the Effect of Cooling Air on Two-Stage Turbine Performance. NASA TM X-1728, 1969.

8. Prust, Herman W., Jr.: An Analytical Study of the Effect of Coolant Flow Variables on the Kinetic Energy Output of a Cooled Turbine Blade Row. Paper 72-12, AIAA, Jan. 1972.

9. Zweifel, O.: Optimum Blade Pitch for Turbomachines With Special Reference to Blades of Great Curvature. Engineering Digest, vol. 7, no. 11, Nov. 1946, pp. 358-360 and vol. 7, no. 12, Dec. 1946, pp. 381-383.

NASA-Langley, 1972 —— 28 E-6912

1. Report No.	2. Government Accession No.	3. Recipient's Catalog No.
NASA TN D-6960		

4. Title and Subtitle	5. Report Date
COLD-AIR INVESTIGATION OF A TURBINE FOR HIGH-TEMPERATURE-ENGINE APPLICATION IV - TWO-STAGE TURBINE PERFORMANCE	September 1972
	6. Performing Organization Code
7. Author(s)	8. Performing Organization Report No.
Warren J. Whitney, Harold J. Schum, and Frank P. Behning	E-6912
	10. Work Unit No.
	764-74
9. Performing Organization Name and Address	11. Contract or Grant No.
Lewis Research Center National Aeronautics and Space Administration Cleveland, Ohio 44135	
	13. Type of Report and Period Covered
12. Sponsoring Agency Name and Address	Technical Note
National Aeronautics and Space Administration Washington, D.C. 20546	14. Sponsoring Agency Code

15. Supplementary Notes

16. Abstract

The two-stage turbine efficiency was 0.932 for equivalent design operating conditions (speed and specific work), which compares closely to the value of 0.929 that would be estimated using the first-stage efficiency. The mass flow obtained with the two-stage configuration indicated that the mass flow characteristics of the two stages were closely matched at design operating conditions. The stage work split at these conditions was 0.505-0.495, which was close to the design work split of 0.515-0.485.

17. Key Words (Suggested by Author(s))	18. Distribution Statement
Turbine aerodynamics High temperature engines	Unclassified - unlimited

19. Security Classif. (of this report)	20. Security Classif. (of this page)	21. No. of Pages	22. Price*
Unclassified	Unclassified	26	$3.00

* For sale by the National Technical Information Service, Springfield, Virginia 22151

"The aeronautical and space activities of the United States shall be conducted so as to contribute . . . to the expansion of human knowledge of phenomena in the atmosphere and space. The Administration shall provide for the widest practicable and appropriate dissemination of information concerning its activities and the results thereof."

— NATIONAL AERONAUTICS AND SPACE ACT OF 1958

NASA SCIENTIFIC AND TECHNICAL PUBLICATIONS

TECHNICAL REPORTS: Scientific and technical information considered important, complete, and a lasting contribution to existing knowledge.

TECHNICAL NOTES: Information less broad in scope but nevertheless of importance as a contribution to existing knowledge.

TECHNICAL MEMORANDUMS: Information receiving limited distribution because of preliminary data, security classification, or other reasons.

CONTRACTOR REPORTS: Scientific and technical information generated under a NASA contract or grant and considered an important contribution to existing knowledge.

TECHNICAL TRANSLATIONS: Information published in a foreign language considered to merit NASA distribution in English.

SPECIAL PUBLICATIONS: Information derived from or of value to NASA activities. Publications include conference proceedings, monographs, data compilations, handbooks, sourcebooks, and special bibliographies.

TECHNOLOGY UTILIZATION PUBLICATIONS: Information on technology used by NASA that may be of particular interest in commercial and other non-aerospace applications. Publications include Tech Briefs, Technology Utilization Reports and Technology Surveys.

Details on the availability of these publications may be obtained from:

SCIENTIFIC AND TECHNICAL INFORMATION OFFICE

NATIONAL AERONAUTICS AND SPACE ADMINISTRATION

Washington, D.C. 20546